Adiponectin Improves Therapeutic Efficacy of Mesenchymal Stem Cells by Enhancing Their Engraftment and Survival in Peri-infarct Myocardium Through AMPK Pathway

Xiaqiu Tian
Beijing Anzhen Hospital https://orcid.org/0000-0002-6652-0434
Xiao-Song Qian
Beijing Chao-Yang Hospital
Hong Wang
Beijing Anzhen Hospital
Yue-Jin Yang (yangyuejinfw@126.com)

Research

Keywords: Mesenchymal stem cell, adiponectin, acute myocardial infarction, AMPK

Posted Date: February 6th, 2020

DOI: https://doi.org/10.21203/rs.2.22775/v1

Abstract

Background: Poor viability of transplanted mesenchymal stem cells (MSCs)within the ischemic heart has limited their therapeutic potential for cardiac repair. We have recently demonstrated that adiponectin (APN) inhibits the apoptosis of MSCs under hypoxia and serum-deprivation conditionsin vitro. This study investigated whether APN could promote the survival of MSCs in vivoand further contribute to cardiac repair after acute myocardial infarction (AMI), via the adenosine monophosphate-activated protein kinase(AMPK)pathway. Methods: Rats were randomized into six groups: the Sham, AMI control, and 4 other groups that were subjected to AMI followed by treatment with MSCs, APN, APN + MSCs and APN + MSCs + AMPK inhibitor. MSCs labeled with CM-DiI were injected through the jugular vein in 24 hours post AMI. At 4-week after AMI, engraftment of MSCs to the peri-infarct myocardium was evaluated. Cardiac function was assessed using echocardiography and left heart catheterization. Apoptosis and fibrosis were measured with TUNEL and Masson's trichrome staining. H&E staining and immunohistochemistry against CD 68 and CD 206 were performed to assess the infiltration of inflammatory cells. Expressions of inflammatory cytokines were determined with ELISA. Immunostaining against smooth muscle cell marker α-smooth-muscle actin (α-SMA) and endothelial cell marker CD31 antibodies were performed to assess arteriogenesis and angiogenesis. Results: APN treatment significantly enhanced the engraftment and survival rate of transplanted MSCs accompanied by markedly improved cardiac function and decreased infarct size at 4-week after AMI. Combined administration of APN and MSCs markedly suppressed inflammatory response, specifically promoted shift of infiltrated macrophages to anti-inflammatory phenotype.Combined administration of APN and MSCs also significantly inhibited cardiomyocytes apoptosis, while increased arteriogenesis and angiogenesis in the peri-infarct myocardium when compared with MSCs transplantation alone. These protective effects of APN were associated with AMPK phosphorylation, which were almost completely reversed by AMPK pathway inhibitor. Conclusions: Our results demonstrated that APN could improve the survival and therapeutic efficacy of transplanted MSCs after AMI through AMPK activation.Our study suggests the potential application of APN for improvement of stem cell-based heart repair and regeneration.

Introduction

Stem cells therapy has been recognized as an attractive therapeutic option to treat cardiovascular diseases during the past decades [1–3]. Among them, mesenchymal stem cells (MSCs) were among the most promising cell types due to their ability to help repair the injured heart via multiple mechanisms [4, 5]. However, data indicated that there appeared to be slight improvement of left ventricular ejection fraction (LVEF) after stem cells transplantation for acute myocardial infarction (AMI) [6, 7]. This was probably attributed to the limited engraftment and poor survival of transplanted MSCs after being exposed to the hostile environment including inflammation [8], various pro-apoptotic factors and low vascularization [9, 10]. Hence, developing strategies to attenuate the hostile environment and promote MSCs engraftment and survival are paramount to enhance the effectiveness of cell therapy for myocardial infarction [11].

Adiponectin (APN) is an adipokine with pleiotropic cardioprotective effects [12, 13], which indicates great potential of improving the myocardial environment after AMI. Moreover, it has recently been proposed to participate in tissue regeneration and promote the survival of several stem cells [14–16], including the proliferation and migration of MSCs [17]. Most importantly, our recent study has verified that APN inhibits the apoptosis of MSCs induced by hypoxia and serum deprivation, which mimics the ischemic conditions in vitro, via the adenosine monophosphate-activated protein kinase (AMPK) pathway [18]. So, in the present study, we further investigated the effect of APN on the survival and therapeutic efficacy of MSCs in vivo in a rat model of AMI, and the role AMPK played in the process.

Material And Methods

Ethics statement

This study was performed in strict accordance with the Chinese guidelines for the care and use of laboratory animals. All animals received humane care and the experimental protocol was approved by the Care of Experimental Animals Committee of Beijing Anzhen Hospital.

Animals and grouping

A total of 85 Sprague-Dawley rats were randomized into six groups: Sham operation (Sham) (n=10), the AMI control (AMI) (n=15), the APN injection only group (APN) (n=15), the MSCs transplantation only group (MSCs) (n=15), the APN combined with MSCs group (APN + MSCs) (n=15) and the additional use of AMPK inhibitor Compound C group (APN + MSCs + AMPK inhibitor) (n=15). MSCs labeled with CM-Dil were injected through the jugular vein in 24 hours post AMI. Globular APN (1 μg/g/d, Biovision, USA) was administered daily intraperitoneally from 20 minutes after AMI for a week, as described previously [19]. Compound C (20 μg/g/d, Selleckchem, USA) were injected intraperitoneally once a day from 20 minutes after AMI until the end of the study.

MSCs isolation, culture and delivery

Isolation and culture of adult rat bone marrow MSCs were performed as previously described [20]. In brief, bone marrow was harvested from the tibia and femur of Sprague-Dawley rats (60-80g, male) and plated into cell culture flasks with complete medium in an incubator set at 37 °C containing 5% CO2 and 95% air. The complete medium was consisted of Iscove's Modified Dulbecco's Medium (IMDM, Gibco, USA), 10% fetal bovine serum (Gibco, USA) and 1% penicillin-streptomycin (Gibco, USA). The d-glucose (dextrose) concentration of IMDM is 25mM. All cells used in the experiment were passage 3.

Prior to transplantation, MSCs were labeled with CellTracker CM-Dil (Molecular Probe, Invitrogen, USA). 2.0×10^6 CM-Dil-labeled MSCs in a total volume of 0.5ml phosphate-buffered saline (PBS) were injected through the tail vein 1-week post AMI as described previously [21]. The control group received the same volume of cell-free PBS.

Establishment of acute myocardial infarction model

The AMI model was established as previously described [22]. Briefly, AMI was induced by permanent ligation of the proximal left anterior descending coronary artery (LAD) with a 6-0 polyester suture 1-2 mm from the tip of the left atrial appendage. The sham-operation group received the same procedure without coronary ligation.

Detection of MSCs engraftment and survival

To explore the role of APN on MSCs survival following intravenous infusion, the hearts were harvested at 4-week after AMI. Hearts were embedded in Tissue-Tek OCT compound (Sakura) and cut into 5 mm-thick serial sections, and nuclei were stained with DAPI. The sections were analyzed using a laser scanning confocal microscope (Leica, Germany). The excitation wavelengths were 561 nm and 405 nm for detection of CM-DiI and DAPI. The numbers of labeled MSCs were quantified by an independent blinded researcher in 10 randomized high-power fields (600 ×) per animal.

Assessment of cardiac function by echocardiography and catheterization

Transthoracic echocardiography was performed at 1-week (baseline) and 4-week (endpoint) after AMI with a 12-MHz phased-array transducer (Sonos 7500, Phillips). After two-dimensional images were obtained, the hearts were measured in M-mode from the parasternal long axis view at the papillary muscle level. The left ventricular end-systolic diameter (LVESd) and end-diastolic diameter (LVEDd) were detected. Left ventricular ejection fraction (LVEF) and left ventricular fractional shortening (LVFS) were calculated using the follows equations: LVEF (%) = $(LVEDd)^3 - (LVESd)^3]/(LVEDd)^3 \times 100\%$, and LVFS (%) = (LVEDd − LVESd)/ LVEDd × 100%. Variations of LVEF and LVFS were calculated as the number of endpoint deducting that of baseline.

Left heart catheterization was performed at 4-week after AMI to assess cardiac function. The left ventricular pressure curve was recorded, and the data of the left ventricular end-diastolic pressure (LVEDP), as well as the left ventricular pressure maximal rate of rise and fall ($\pm dp/dt_{max}$) were recorded.

Histological assessment of infarct size and inflammation

At 4-week post AMI, the animals were sacrificed, and the heart tissues were collected. The hearts were fixed in 10% formalin for the preparation of paraffin sections. The paraffin sections were stained with Masson's trichrome and Hematoxylin-Eosin (H&E). The infarct sizes are expressed as percentages of the total left ventricular areas (fibrotic area/total left ventricular area × 100%). H&E staining was performed to evaluate the degree of neutrophils infiltration. The densities of neutrophils in the peri-infarct myocardium were determined from 10 randomly selected areas in a blinded fashion based on morphology of nuclei and cell size, as described previously [23]. To further evaluate the level and phenotype of macrophages infiltration, immunohistochemistry against CD68 (M1 marker) and CD206 (M2 marker) were performed. The sections were processed as aforementioned histological procedure and incubated overnight with

primary rabbit anti-CD68 (Abcam, 1:1,000 dilution) and CD206 (Abcam, 1:1,000 dilution) antibodies at 4°C followed by incubation with the goat anti-rabbit IgG (Beyotime, China, 1:200 dilution) secondary antibody and color reaction with the DAB kit. The stained sections were examined under microscope in 5 high-power fields (HPF) randomly chosen fields. The results of inflammatory cells infiltration were described as follows: the number of neutrophils / mm^2, $CD68^+$ cells / HPF and $CD206^+$ cells / HPF.

Assessment of cardiomyocytes and MSCs' apoptosis with TUNEL assay

For apoptosis analysis, TdT-mediated dUTP nick-end labeling (TUNEL) In Situ Cell Death Detection (Roche, Mannheim, Germany, 11772465001) was performed according to the manufacture's instruction. The samples were fixed in OCT medium. TUNEL-positive cells were examined under fluorescence microscope at 200 × magnification in 5 randomly chosen fields. Nuclei were stained with DAPI and presented as blue color while apoptotic nuclei were green. The results were presented as the percentage of apoptotic cells / total cells.

Determination of pro- and anti-inflammatory cytokines in heart tissues with ELISA

Quantitative immunoassay was used for evaluating expressions of interleukin-6 (IL-6), tumor necrosis factor-α (TNF-α) and interleukin-10 (IL-10) in peri-infarct area at the endpoint according to manufacturer's protocol (R&D Systems, USA). Tissues from the peri-infarct regions of myocardium were homogenized. IL-6, TNF-α and IL-10 supplied by the kit were used to plot standard curve. Optical density of each sample was detected by Enzyme-labeling measuring instrument at the wavelength of 450nm, and the concentration was determined on the standard curve. All the measurements were repeated for 3 times to obtain arithmetic average.

Evaluation of arteriogenesis and angiogenesis using immunohistochemistry and immunofluorescence staining

Immunohistochemistry and immunofluorescence staining were performed to evaluate vessel density in peri-infarct areas. Sections were fixed in 4% paraformaldehyde, rinsed with PBS, and blocked with 0.1% PBS-T containing 1% BSA. The sections were processed as aforementioned histological procedure and incubated overnight with primary rabbit anti-α-smooth muscle actin (α-SMA, Abcam, 1:1,000 dilution) antibodies at 4°C followed by incubation with the goat anti-rabbit IgG (Beyotime, China, 1:200 dilution) secondary antibody and color reaction with the DAB kit. After co-incubated with rabbit anti-CD31 (1:300, Abcam, Cambridge, MA) at 4°C overnight, sections were washed with PBS, and co-incubated with goat anti-rabbit Alexa Fluor 488 (Cell Signaling Technology, Danvers, MA, #4412, 1:500) secondary antibody (R&D systems, Minneapolis, MN, NL007, 1:100). After washing, the nuclei were counterstained with DAPI (Invitrogen). The sections were analyzed under a laser scanning confocal microscope FV1000 (Olympus) and 5 random high-power fields were chosen per animal.

Detection of AMPK phosphorylation with Western blot analysis

Tissues were extracted from peri-infarct regions of the myocardium. Protein concentrations were measured with a BCA assay. To detect the expression of AMPK and phospho-AMPK (p-AMPK) in the heart tissue, 50 mg of protein lysate was resolved by SDS-PAGE, transferred to nitrocellulose membranes (Life Technologies), and blocked with 5% non-fat dry milk. The primary antibodies used were as follows: β-actin (1:1000, Cell Signaling Technology, Danvers, MA), AMPK (1:1000, Cell Signaling Technology, Danvers, MA) and p-AMPK (1:1000, Cell Signaling Technology, Danvers, MA). Target protein signals were normalized to β-actin as a loading control (1:1000 dilution; Zhongshanjinqiao, China). After washing, the membranes were incubated for 1 h at room temperature in blocking solution containing the peroxidase-conjugated secondary antibodies. Next, the membranes were washed and processed for analysis using a Chemiluminescence Detection Kit (Pierce) according to the manufacturer's instructions. Densitometry analysis was completed using Quantity One software.

Statistics

All the data were described as mean ± SD, and analyses were performed with GraphPad Prism software (Version 6.0c, GraphPad Software, La Jolla, CA). Statistical significance among groups was evaluated with One Way ANOVA followed by post hoc LSD-test, and a value of $p < 0.05$ was considered statistically significant.

Results

APN treatment facilitated the engraftment and survival of MSCs in peri-infarct myocardium

In accordance with the protective effect of APN on MSCs *in vitro* observed in our previous study, APN treatment improves the engraftment and survival of transplanted MSCs *in vivo* at 4-week after infarction. As shown in **Figure 1**, there were few CM-DiI positive cells in the border zone of ischemic myocardium in rats treated with MSCs-only. In comparison, the combined administration of APN and MSCs markedly increased CM-DiI positive cells in the peri-infarct myocardium (15.78 ± 2.88% vs. 8.02 ± 2.26%, $p < 0.05$), suggesting that APN treatment might increase the engraftment and survival potential of transplanted MSCs in post-infarct cardiac tissue.

APN adjuvant with MSCs treatment improved cardiac function and attenuated adverse remodeling

According to the cardiac dimensions and function results assessed with echocardiography, the AMI rats did not exhibit any differences at the baseline in different groups, validating the reliability and consistency of the established AMI models (**Table S1**). At 4-week post AMI, the rats in MSCs-only group demonstrated significantly enhanced value of change in LVEF (ΔLVEF) and LVFS (ΔLVFS), compared with those in the AMI control group. Compared with MSC-only treated group, APN combined with MSCs (APN + MSCs) treatment induced a more significant improvement in LVEF (8.77 ± 2.32% vs. 5.32 ± 2.99% by MSCs treatment, $p < 0.05$) and LVFS (5.10 ± 1.45% vs. 2.97 ± 1.68% by MSCs treatment, $p < 0.05$) (**Figure 2A and 2B**). Moreover, rats in APN + MSCs group also exhibited significantly reduced values of change in LVEDd (ΔLVEDd) and LVESd (ΔLVESd) (**Figure 2C and 2D**), indicating the attenuation of

ventricular structural remodeling. In addition, the left heart catheterization results revealed that combination regimen of APN and MSCs resulted in a significantly reduced LVEDP and increase in $+dp/dt_{max}$ and $-dp/dt_{max}$ in comparison with MSCs-only treatment (**Figure 2E-2G**, **Table S2**).

APN adjuvant with MSCs treatment reduced myocardial infarct size

We performed Masson's trichrome staining of the heart tissue at 4-week after infarction. As shown in **Figure 3**, transmural infarction existed in all groups of rats developed with AMI model. There were thinning anterior wall, dilated LV chamber, severe fibrosis and large infarct size in the hearts of AMI control rats. Compared with AMI control group, there were smaller infarct size in the hearts of both APN (25.79 ± 2.42% vs. 37.95 ± 5.12%, $p < 0.05$) and MSCs-treated rats (27.87 ± 1.88% vs. 37.95 ± 5.12%, $p < 0.05$). The combined delivery of APN and MSCs reduced the infarct size to a larger extent compared with MSCs transplantation alone (21.38 ± 3.57% vs. 27.87 ± 1.88%, $p < 0.05$).

APN adjuvant with MSCs treatment inhibited inflammation in peri-infarct myocardium

We performed histological analysis at 4-week after infarction to assess the infiltration of inflammatory cells (**Figure 4, Table S3**). As shown in **Figure 4A**, H&E staining and immunohistochemistry (IHC) demonstrated massive infiltration of neutrophils and $CD68^+$ macrophages in peri-infarct region in the AMI group, which was inhibited by MSCs- or APN- alone treatment ($p < 0.05$). The combined therapy of APN + MSCs further significantly reduced neutrophils (13.57 ± 4.60 vs. 24.10 ± 2.55, $p < 0.05$) and $CD68^+$ macrophages infiltration (16.00 ± 6.22 vs. 34.71 ± 7.09, $p < 0.05$) compared with MSCs treatment alone (**Figure 4B, 4C**). In comparison, IHC staining with CD206 showed that MSCs significantly increased the number of CD 206^+ macrophages in the peri-infarct region compared with AMI group ($p < 0.05$), while combined regimen of APN + MSCs further increased the $CD206^+$ macrophages compared with MSCs-only group (117.70 ± 27.99 vs. 85.55 ± 13.48, $p < 0.05$) (**Figure 4A, 4D**). To further quantitatively assess the inflammatory response, we measured the levels of inflammatory cytokines in the myocardial tissues by ELISA. As shown in **Figure 4E to 4G**, compared with AMI group, the administration of MSCs effectively reduced the levels of pro-inflammatory cytokines IL-6 and TNF-α, while increased the level of anti-inflammatory cytokine IL-10 in peri-infarct myocardium ($p < 0.05$). Combined administration of APN and MSCs further significantly decreased the expression of IL-6 (8.90 ± 1.51 pg/mg vs. 4.31 ± 3.82 pg/mg, $p < 0.05$) and TNF-α (5.29 ± 1.26 pg/mg vs. 9.39 ± 0.63 pg/mg, $p < 0.05$), and increased the level of IL-10 (12.29 ± 2.20 pg/mg vs. 9.40 ± 0.65 pg/mg, $p < 0.05$) in comparison with MSCs treatment alone.

APN adjuvant with MSCs treatment inhibited cardiomyocytes and MSCs' apoptosis in peri-infarct region

We performed TUNEL staining to evaluate the apoptosis of cardiomyocytes and transplanted MSCs. As shown in **Figure 5A and 5B**, AMI-induced cardiomyocytes apoptosis at the border zone of infarct myocardium was significantly reduced with the transplantation of MSCs ($p < 0.05$). Administration of APN alone was also associated with a decline of apoptotic cardiomyocytes in the peri-infarct myocardium ($p < 0.05$). Combined therapy with APN and MSCs, with greatly improved engraftment of

MSCs, induced a more significant reduction in the number of apoptotic cardiomyocytes compared with MSC-only group (13.57 ± 4.60% vs. 24.10 ± 2.55%, $p < 0.05$). Notably, in line with the anti-apoptotic effect of APN on MSCs *in vitro*, TUNEL results also showed a significant reduction of apoptosis of transplanted MSCs in APN + MSCs group compared with MSCs-only group *in vivo* (27.57 ± 3.95% vs. 38.30 ± 4.98%, $p < 0.05$) (**Figure 5C**).

APN adjuvant with MSCs treatment enhanced arteriogenesis and angiogenesis in peri-infarct myocardium

Immunostaining against smooth muscle cell marker α-smooth-muscle actin (α-SMA) and endothelial cell marker CD31 antibodies were performed at 4-week after AMI to assess arteriogenesis and angiogenesis in peri-infarct myocardium, respectively. As shown in **Figure 6**, the number of both α-SMA and CD 31 positive vessels in MSCs transplantation group were markedly enhanced compared with AMI group ($p < 0.05$). Moreover, combined administration of APN and MSCs further improved α-SMA (13.80 ± 3.11 vs. 7.60 ± 1.52, $p < 0.05$) and CD 31 positive vessels (23.20 ± 6.06 vs. 12.80 ± 1.48, $p < 0.05$) compared with MSCs transplantation alone.

APN enhanced the therapeutic effect of MSCs transplantation through the AMPK pathway

As shown in **Figure 7**, APN significantly increased the phosphorylation of AMPK in the peri-infarct myocardium. The combined therapy with APN and MSCs further activated AMPK phosphorylation, which could be markedly reversed by AMPK inhibitor, compound C. Further, we found that the improved survival of MSCs brought by APN was attenuated with the administration of compound C ($p < 0.05$), which implied the potential role of AMPK played in this process. More importantly, the beneficial effects of APN + MSCs on cardiac function recovery, infarct size reduction, anti-inflammatory and anti-apoptotic effects, and enhancement of arteriogenesis and angiogenesis were all markedly diminished with the administration of the AMPK-inhibitor (**Figure 1 – 6, Table S4**), indicating that these abovementioned beneficial effects of APN + MSCs treatment were mainly attributed to AMPK pathway activation.

Discussion

Our present study provides novel laboratory evidence extending the previous report by showing that APN adjuvant with MSCs transplantation provides a promising strategy for cardiac repair and regeneration after AMI. It has been shown that limited engraftment and poor survival rate of transplanted MSCs in peri-infarct myocardium are the primary barriers that limit the effectiveness of cell therapy [8–10]. On the basis of our recent in vitro study showing APN inhibits the apoptosis of MSCs induced by hypoxia and serum deprivation [18], in this study, we further proved that APN significantly enhanced the survival of transplanted MSCs in the peri-infarct myocardium in vivo, with resultant improved cardiac function, attenuated ventricular remodeling and reduced infarct size. At the cellular level, the underlying mechanisms may involve the inhibition of inflammation, especially the promotion of macrophages change into anti-inflammatory phenotype, the reduction of cardiomyocytes apoptosis, and the increment

of arteriogenesis and angiogenesis in the peri-infarct myocardium. Further, at the molecular level, the above-mentioned beneficial effects were associated with the AMPK pathway activation (Fig. 8).

Besides the well-established metabolic-regulatory and cardioprotective effects, APN was recently found to be a tissue regenerating hormone [14] and participate in promoting the survival of hematopoietic stem cells [15], bone marrow mononuclear cells [24], mesoangioblasts [25] and endothelial progenitor cells [26]. Specifically, APN also has some beneficial effects in terms of MSCs, including facilitating MSCs osteogenesis under osteogenic induction [27, 28], enhancing MSCs resistance to flow shear stress [29] and regulating the mobilization and recruitment of MSCs to participate in tissue repair and regeneration [17, 30]. Most importantly, our recent in vitro experiment has shown that APN promotes the survival of MSCs under the hypoxic and serum deprivation condition, which mimics the ischemic environment [18]. In the field of cardiac repair, recent study has found another adipokine, leptin, also confers anti-apoptotic effect and enhances therapeutic effects of MSCs after myocardial infarction [31]. However, the effects of APN on the survival of MSCs under the hostile microenvironment after infarction and the efficacy of cardiac repair and regeneration have never been investigated so far.

Our present study showed that the engraftment and survival of MSCs in the peri-infarct myocardium were significantly increased with the APN treatment, accompanied with markedly improved cardiac function and decreased infarct size at 4-week after AMI. Compared with the genetic [32–34] and nongenetic modifications [35, 36] employed to enhance stem cell engraftment and survival, we have previously proved that the interventions aimed at improving the quality of local microenvironments to facilitate survival and biological behavior of transplanted cells are similarly effective and clinically practicable [20–23, 37–40].

In addition, the present study revealed that the remarkable beneficial effects of APN on MSCs survival and the following cardiac repairs were mediated by the activation of AMPK, which correlates well with our in vitro study that AMPK mediated the inhibitory effects of APN on the apoptosis of MSCs [18]. The activation of AMPK by APN is critical in cellular responses to metabolic stress involving energy generation and consumption [19, 41–43], thus mediating the protective effects of APN on the survival of MSCs [18, 29]. Our data revealed that APN induced sustained phosphorylation of AMPK in myocardium at 4-week post AMI, and the application of inhibitors of AMPK significantly inhibited the protective effect offered by APN. Taken together, these findings strongly indicate that AMPK pathway is critically required in the protective actions of APN on MSCs survival and cardiac repair. This is the first attempt to elucidate the signals involved in APN-mediated protective properties in MSCs under infarcted myocardial microenvironment.

Furthermore, the present study has found that the cellular mechanisms underlying the striking therapeutic effects are mainly associated with anti-inflammation, anti-apoptosis activity, and enhancement of arteriogenesis and angiogenesis by synergism of APN and MSC transplantation.

Post-myocardial wound healing consists of a number of complex inflammatory events that are both time- and cell-type-dependent. Neutrophils and macrophages infiltrate injured tissue in large numbers early

after ischemia and participate in tissue repair. In particular, polarization of macrophages (a proper shift toward M2 macrophages) would help to prevent excessive scar formation and remodeling, and may have significant clinical implications attenuating inflammatory cytokines [44, 45]. In recent years, it has become clear that the therapeutic properties of stem cells are related to their capacity to modulate the inflammatory and immune response [5, 46–48]. A previous study has demonstrated that MSCs switch macrophages into a regulatory phenotype characterized by increased expression levels of IL-10 and reduced levels of TNF-α in vitro [49]. A recent in vivo study also showed that MSCs might promote the phenotype of the infiltrated macrophages shift to anti-inflammatory M2 and modulate the immunologic environment after myocardial infarction [50]. In line with these studies, our present study also demonstrated that MSCs transplantation increased the number of M2 ($CD206^+$) macrophages, while combined administration of APN and MSCs further improved the macrophages shift to M2 phenotype. These results were confirmed by the decrease of inflammatory cytokines IL-6 and TNF-α, and an elevation of anti-inflammatory cytokine IL-10. It is reasonable to believe that the modification of the cytokine-rich unfavorable environment by regulation of the balance between M1 and M2 macrophages may result in a promoted survival of therapeutic MSCs.

Besides, both MSCs and APN were shown to protect cardiomyocyte from apoptosis [41, 51], which is the main contributor of the massive cardiomyocytes death in the infarcted heart. Consistent with these findings, we demonstrated in this study that both MSCs and APN treatment decreased the number of apoptotic cardiomyocytes in peri-infarct myocardium, while APN adjuvant with MSC could further profoundly suppress apoptosis. Of particular note, our results also showed a significant reduction of apoptosis of transplanted MSCs in APN combined with MSCs group compared with MSCs-only group, which is in consistency with our previous study demonstrated that APN inhibited the apoptosis of MSCs under hypoxia and serum-deprivation conditions in vitro. In addition, the maintenance of vessel density led to the preservation of cardiac function and protection against the ventricular remodeling in AMI model. Pro-angiogenesis is a well-known paracrine mechanism through which MSCs exert cardioprotective effect [52]. APN also has pro-angiogenesis effect, which might be attributable to enhanced migration and function of endothelial progenitor cells [26, 53]. In this study, we also found that APN adjuvant with MSCs treatment promoted arteriogenesis and angiogenesis in peri-infarct regions, which could further help to repair the damaged heart.

Conclusion

In conclusion, for the first time, this study has documented experimental evidence showing that a combination of APN and MSCs transplantation may have a synergism in regeneration and repair of myocardial function and morphology post-infarction. APN treatment could effectively enhance survival of transplanted MSCs in the infarcted tissue, accompanied by functional benefits resulting from cell transplantation. The data from the present study suggest APN + MSCs combination regimen as a promising strategy for the further improvement of the clinical therapeutic efficacy of MSCs in patients with AMI.

Abbreviations

MSCs
mesenchymal stem cells
APN
adiponectin
AMI
acute myocardial infarction
AMPK
adenosine monophosphate-activated protein kinase
LVEF
left ventricular ejection fraction
IMDM
Iscove's Modified Dulbecco's Medium
PBS
phosphate-buffered saline
LAD
left anterior descending coronary artery
LVESd
left ventricular end-systolic diameter
LVEDd
left ventricular end-diastolic diameter
LVFS
left ventricular fractional shortening
LVEDP
left ventricular end-diastolic pressure
H&E
Hematoxylin-Eosin
TUNEL
TdT-mediated dUTP nick-end labeling
IL
interleukin
TNF-α
tumor necrosis factor-α
α-SMA
α-smooth muscle actin
IHC
immunohistochemistry
NE
neutrophils

HPF
high power field
CM-DiI
1,1’-dioctadecyl-3,3,3’,3’-tetramethylindocarbocyanine perchlorate
DAPI
4’6-diamidino-2-phenylindole dihydrochloride

Declarations

Ethics approval and consent to participate

This study was performed in strict accordance with the Chinese guidelines for the care and use of laboratory animals. All animals received humane care and the experimental protocol was approved by the Care of Experimental Animals Committee of Beijing Anzhen Hospital.

Consent for publication

Not applicable

Availability of data and materials

The datasets used and/or analysed during the current study are available from the corresponding author on reasonable request.

Competing interests

The authors declare that they have no competing interests.

Funding

This work was supported by grants from National Natural Science Foundation of China (81700362, 81300112) and 863 Program of China (2011AA020110).

Authors’ contributions

X.-Q. T.: conception and design, provision of study material or animals, data analysis and interpretation, manuscript writing, final approval of manuscript; X.-S. Q.: provision of study material or animals, final approval of manuscript; H.W.: data analysis and interpretation, manuscript writing, final approval of manuscript; Y.-J. Y.: conception and design, financial support, provision of study material or patients, manuscript writing, final approval of manuscript.

Acknowledgements

Not applicable.

References

1. Desgres M, Menasche P. Clinical Translation of Pluripotent Stem Cell Therapies: Challenges and Considerations. Cell Stem Cell. 2019, 25(5):594-606.
2. Goradel NH, Hour FG, Negahdari B, Malekshahi ZV, Hashemzehi M, Masoudifar A, Mirzaei H. Stem Cell Therapy: A New Therapeutic Option for Cardiovascular Diseases. J Cell Biochem. 2018, 119(1):95-104.
3. Lemcke H, Voronina N, Steinhoff G, David R. Recent Progress in Stem Cell Modification for Cardiac Regeneration. Stem Cells Int. 2018, 2018:1909346.
4. Shafei AE, Ali MA, Ghanem HG, Shehata AI, Abdelgawad AA, Handal HR, Talaat KA, Ashaal AE, El-Shal AS. Mesenchymal stem cell therapy: A promising cell-based therapy for treatment of myocardial infarction. J Gene Med. 2017, 19(12):e2995.
5. Luger D, Lipinski MJ, Westman PC, Glover DK, Dimastromatteo J, Frias JC, Albelda MT, Sikora S, Kharazi A, Vertelov G *et al*. Intravenously Delivered Mesenchymal Stem Cells: Systemic Anti-Inflammatory Effects Improve Left Ventricular Dysfunction in Acute Myocardial Infarction and Ischemic Cardiomyopathy. Circ Res. 2017, 120(10):1598-613.
6. Afzal MR, Samanta A, Shah ZI, Jeevanantham V, Abdel-Latif A, Zuba-Surma EK, Dawn B. Adult Bone Marrow Cell Therapy for Ischemic Heart Disease: Evidence and Insights From Randomized Controlled Trials. Circ Res. 2015, 117(6):558-75.
7. Liu B, Duan CY, Luo CF, Ou CW, Sun K, Wu ZY, Huang H, Cheng CF, Li YP, Chen MS. Effectiveness and safety of selected bone marrow stem cells on left ventricular function in patients with acute myocardial infarction: a meta-analysis of randomized controlled trials. Int J Cardiol. 2014, 177(3):764-70.
8. Khodayari S, Khodayari H, Amiri AZ, Eslami M, Farhud D, Hescheler J, Nayernia K. Inflammatory Microenvironment of Acute Myocardial Infarction Prevents Regeneration of Heart with Stem Cells Therapy. Cell Physiol Biochem. 2019, 53(5):887-909.
9. Hu X, Xu Y, Zhong Z, Wu Y, Zhao J, Wang Y, Cheng H, Kong M, Zhang F, Chen Q *et al*. A Large-Scale Investigation of Hypoxia-Preconditioned Allogeneic Mesenchymal Stem Cells for Myocardial Repair in Nonhuman Primates: Paracrine Activity Without Remuscularization. Circ Res. 2016, 118(6):970-83.
10. Sanganalmath SK, Bolli R. Cell therapy for heart failure: a comprehensive overview of experimental and clinical studies, current challenges, and future directions. Circ Res. 2013, 113(6):810-34.
11. Taylor DA, Chandler AM, Gobin AS, Sampaio LC. Maximizing Cardiac Repair: Should We Focus on the Cells or on the Matrix? Circ Res. 2017, 120(1):30-32.
12. Achari AE, Jain SK. Adiponectin, a Therapeutic Target for Obesity, Diabetes, and Endothelial Dysfunction. Int J Mol Sci. 2017, 18(6):e1321.
13. Fang H, Judd RL. Adiponectin Regulation and Function. Compr Physiol. 2018, 8(3):1031-63.
14. Fiaschi T, Magherini F, Gamberi T, Modesti PA, Modesti A. Adiponectin as a tissue regenerating hormone: more than a metabolic function. Cell Mol Life Sci. 2014, 71(10):1917-25.

15. Masamoto Y, Arai S, Sato T, Kubota N, Takamoto I, Kadowaki T, Kurokawa M. Adiponectin Enhances Quiescence Exit of Murine Hematopoietic Stem Cells and Hematopoietic Recovery Through mTORC1 Potentiation. Stem Cells. 2017, 35(7):1835-48.
16. Ren Y, Li Y, Yan J, Ma M, Zhou D, Xue Z, Zhang Z, Liu H, Yang H, Jia L *et al*. Adiponectin modulates oxidative stress-induced mitophagy and protects C2C12 myoblasts against apoptosis. Sci Rep. 2017, 7(1):3209.
17. Yu L, Tu Q, Han Q, Zhang L, Sui L, Zheng L, Meng S, Tang Y, Xuan D, Zhang J *et al*. Adiponectin regulates bone marrow mesenchymal stem cell niche through a unique signal transduction pathway: an approach for treating bone disease in diabetes. Stem Cells. 2015, 33(1):240-52.
18. Tian XQ, Yang YJ, Li Q, Huang PS, Li XD, Jin C, Qi K, Jiang LP, Chen GH. Globular Adiponectin Inhibits the Apoptosis of Mesenchymal Stem Cells Induced by Hypoxia and Serum Deprivation via the AdipoR1-Mediated Pathway. Cell Physiol Biochem. 2016, 38(3):909-25.
19. Yan W, Zhang H, Liu P, Wang H, Liu J, Gao C, Liu Y, Lian K, Yang L, Sun L *et al*. Impaired mitochondrial biogenesis due to dysfunctional adiponectin-AMPK-PGC-1alpha signaling contributing to increased vulnerability in diabetic heart. Basic Res Cardiol. 2013, 108(3):329.
20. Xu J, Xiong YY, Li Q, Hu MJ, Huang PS, Xu JY, Tian XQ, Jin C, Liu JD, Qian L *et al*. Optimization of Timing and Times for Administration of Atorvastatin-Pretreated Mesenchymal Stem Cells in a Preclinical Model of Acute Myocardial Infarction. Stem Cells Transl Med. 2019, 8(10):1068-83.
21. Tian XQ, Yang YJ, Li Q, Xu J, Huang PS, Xiong YY, Li XD, Jin C, Qi K, Jiang LP *et al*. Combined therapy with atorvastatin and atorvastatin-pretreated mesenchymal stem cells enhances cardiac performance after acute myocardial infarction by activating SDF-1/CXCR4 axis. Am J Transl Res. 2019, 11(7):4214-31.
22. Zhang Q, Wang H, Yang YJ, Dong QT, Wang TJ, Qian HY, Li N, Wang XM, Jin C. Atorvastatin treatment improves the effects of mesenchymal stem cell transplantation on acute myocardial infarction: the role of the RhoA/ROCK/ERK pathway. Int J Cardiol. 2014, 176(3):670-9.
23. Yang YJ, Qian HY, Huang J, Li JJ, Gao RL, Dou KF, Yang GS, Willerson JT, Geng YJ. Combined therapy with simvastatin and bone marrow-derived mesenchymal stem cells increases benefits in infarcted swine hearts. Arterioscler Thromb Vasc Biol. 2009, 29(12):2076-82.
24. Eren P, Camus S, Matrone G, Ebrahimian TG, Francois D, Tedgui A, Sebastien Silvestre J, Blanc-Brude OP. Adiponectinemia controls pro-angiogenic cell therapy. Stem Cells. 2009, 27(11):2712-21.
25. Fiaschi T, Tedesco FS, Giannoni E, Diaz-Manera J, Parri M, Cossu G, Chiarugi P. Globular adiponectin as a complete mesoangioblast regulator: role in proliferation, survival, motility, and skeletal muscle differentiation. Mol Biol Cell. 2010, 21(6):848-59.
26. Huang PH, Chen JS, Tsai HY, Chen YH, Lin FY, Leu HB, Wu TC, Lin SJ, Chen JW. Globular adiponectin improves high glucose-suppressed endothelial progenitor cell function through endothelial nitric oxide synthase dependent mechanisms. J Mol Cell Cardiol. 2011, 51(1):109-19.
27. Pu Y, Wu H, Lu S, Hu H, Li D, Wu Y, Tang Z. Adiponectin Promotes Human Jaw Bone Marrow Stem Cell Osteogenesis. J Dent Res. 2016, 95(7):769-75.

28. Wang Y, Zhang X, Shao J, Liu H, Liu X, Luo E. Adiponectin regulates BMSC osteogenic differentiation and osteogenesis through the Wnt/beta-catenin pathway. Sci Rep. 2017, 7(1):3652.
29. Zhao L, Fan C, Zhang Y, Yang Y, Wang D, Deng C, Hu W, Ma Z, Jiang S, Di S *et al*. Adiponectin enhances bone marrow mesenchymal stem cell resistance to flow shear stress through AMP-activated protein kinase signaling. Sci Rep. 2016, 6:28752.
30. Pu Y, Wang M, Hong Y, Wu Y, Tang Z. Adiponectin promotes human jaw bone marrow mesenchymal stem cell chemotaxis via CXCL1 and CXCL8. J Cell Mol Med. 2017, 21(7):1411-19.
31. Yang F, Wu R, Jiang Z, Chen J, Nan J, Su S, Zhang N, Wang C, Zhao J, Ni C *et al*. Leptin increases mitochondrial OPA1 via GSK3-mediated OMA1 ubiquitination to enhance therapeutic effects of mesenchymal stem cell transplantation. Cell Death Dis. 2018, 9(5):556.
32. Cornu TI, Mussolino C, Cathomen T. Refining strategies to translate genome editing to the clinic. Nat Med. 2017, 23(4):415-23.
33. Tam C, Wong JH, Cheung RCF, Zuo T, Ng TB. Therapeutic potentials of short interfering RNAs. Appl Microbiol Biotechnol. 2017, 101(19):7091-111.
34. Wu Z, Chen G, Zhang J, Hua Y, Li J, Liu B, Huang A, Li H, Chen M, Ou C. Treatment of Myocardial Infarction with Gene-modified Mesenchymal Stem Cells in a Small Molecular Hydrogel. Sci Rep. 2017, 7(1):15826.
35. Huang P, Tian X, Li Q, Yang Y. New strategies for improving stem cell therapy in ischemic heart disease. Heart Fail Rev. 2016, 21(6):737-52.
36. Park SJ, Kim RY, Park BW, Lee S, Choi SW, Park JH, Choi JJ, Kim SW, Jang J, Cho DW *et al*. Dual stem cell therapy synergistically improves cardiac function and vascular regeneration following myocardial infarction. Nat Commun. 2019, 10(1):3123.
37. Ezquer FE, Ezquer ME, Vicencio JM, Calligaris SD. Two complementary strategies to improve cell engraftment in mesenchymal stem cell-based therapy: Increasing transplanted cell resistance and increasing tissue receptivity. Cell Adh Migr. 2017, 11(1):110-19.
38. Yang YJ, Qian HY, Huang J, Geng YJ, Gao RL, Dou KF, Yang GS, Li JJ, Shen R, He ZX *et al*. Atorvastatin treatment improves survival and effects of implanted mesenchymal stem cells in post-infarct swine hearts. Eur Heart J. 2008, 29(12):1578-90.
39. Song L, Yang YJ, Dong QT, Qian HY, Gao RL, Qiao SB, Shen R, He ZX, Lu MJ, Zhao SH *et al*. Atorvastatin enhance efficacy of mesenchymal stem cells treatment for swine myocardial infarction via activation of nitric oxide synthase. PLoS One. 2013, 8(5):e65702.
40. Xu JY, Qian HY, Huang PS, Xu J, Xiong YY, Jiang WY, Xu Y, Leng WX, Li XD, Chen GH *et al*. Transplantation efficacy of autologous bone marrow mesenchymal stem cells combined with atorvastatin for acute myocardial infarction (TEAM-AMI): rationale and design of a randomized, double-blind, placebo-controlled, multi-center, Phase II TEAM-AMI trial. Regen Med. 2019.
41. Konishi M, Haraguchi G, Ohigashi H, Ishihara T, Saito K, Nakano Y, Isobe M. Adiponectin protects against doxorubicin-induced cardiomyopathy by anti-apoptotic effects through AMPK up-regulation. Cardiovasc Res. 2011, 89(2):309-19.

42. Huang B, Cheng X, Wang D, Peng M, Xue Z, Da Y, Zhang N, Yao Z, Li M, Xu A *et al*. Adiponectin promotes pancreatic cancer progression by inhibiting apoptosis via the activation of AMPK/Sirt1/PGC-1alpha signaling. Oncotarget. 2014, 5(13):4732-45.
43. Iwabu M, Yamauchi T, Okada-Iwabu M, Sato K, Nakagawa T, Funata M, Yamaguchi M, Namiki S, Nakayama R, Tabata M *et al*. Adiponectin and AdipoR1 regulate PGC-1alpha and mitochondria by Ca(2+) and AMPK/SIRT1. Nature. 2010, 464(7293):1313-9.
44. Gordon S. Alternative activation of macrophages. Nat Rev Immunol. 2003, 3(1):23-35.
45. Gordon S, Taylor PR. Monocyte and macrophage heterogeneity. Nat Rev Immunol. 2005, 5(12):953-64.
46. Vagnozzi RJ, Maillet M, Sargent MA, Khalil H, Johansen AK, Schwanekamp JA, York AJ, Huang V, Nahrendorf M, Sadayappan S *et al*. An acute immune response underlies the benefit of cardiac stem-cell therapy. Nature. 2019.
47. Huynh K. Stem cell therapy improves heart function by triggering an acute immune response. Nat Rev Cardiol. 2019.
48. Epstein SE, Luger D, Lipinski MJ. Paracrine-Mediated Systemic Anti-Inflammatory Activity of Intravenously Administered Mesenchymal Stem Cells: A Transformative Strategy for Cardiac Stem Cell Therapeutics. Circ Res. 2017, 121(9):1044-46.
49. Maggini J, Mirkin G, Bognanni I, Holmberg J, Piazzon IM, Nepomnaschy I, Costa H, Canones C, Raiden S, Vermeulen M *et al*. Mouse bone marrow-derived mesenchymal stromal cells turn activated macrophages into a regulatory-like profile. PLoS One. 2010, 5(2):e9252.
50. Cho DI, Kim MR, Jeong HY, Jeong HC, Jeong MH, Yoon SH, Kim YS, Ahn Y. Mesenchymal stem cells reciprocally regulate the M1/M2 balance in mouse bone marrow-derived macrophages. Exp Mol Med. 2014, 46:e70.
51. Shibata R, Sato K, Pimentel DR, Takemura Y, Kihara S, Ohashi K, Funahashi T, Ouchi N, Walsh K. Adiponectin protects against myocardial ischemia-reperfusion injury through AMPK- and COX-2-dependent mechanisms. Nat Med. 2005, 11(10):1096-103.
52. Gnecchi M, Zhang Z, Ni A, Dzau VJ. Paracrine mechanisms in adult stem cell signaling and therapy. Circ Res. 2008, 103(11):1204-19.
53. Adams V, Heiker JT, Hollriegel R, Beck EB, Woitek FJ, Erbs S, Bluher M, Stumvoll M, Beck-Sickinger AG, Schuler G *et al*. Adiponectin promotes the migration of circulating angiogenic cells through p38-mediated induction of the CXCR4 receptor. Int J Cardiol. 2013, 167(5):2039-46.

Figures

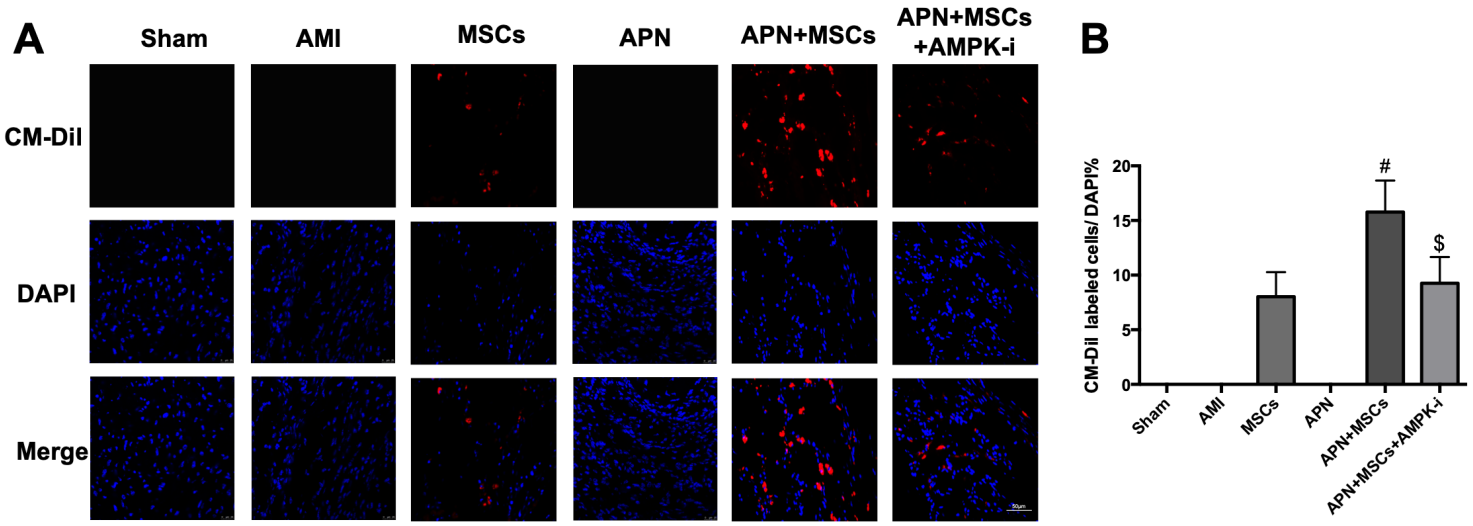

Figure 1

Engraftment and survival of transplanted MSCs labeled with CM-DiI. (A): Representative image of CM-DiI-labeled cells in the peri-infarcted myocardium at the end of 4 weeks post AMI. (B): Quantitation of CM-DiI-labeled cells in the peri-infarcted myocardium per high power field (HPF) in each group. The number of CM-DiI positive cells in the APN + MSCs group was markedly increased compared with MSCs-only group, which was significantly decreased with the treatment of AMPK-inhibitor. n = 10 in each group. # $p < 0.05$ compared with MSCs group; $ $p < 0.05$ compared with APN+MSCs group. AMI: acute myocardial infarction; APN: adiponectin; MSCs: mesenchymal stem cells; AMPK: adenosine monophosphate-activated protein kinase; CM-DiI: 1,1'-dioctadecyl-3,3,3',3'-tetramethylindocarbocyanine perchlorate; DAPI: 4'6-diamidino-2-phenylindole dihydrochloride. Scale bar = 50 μm.

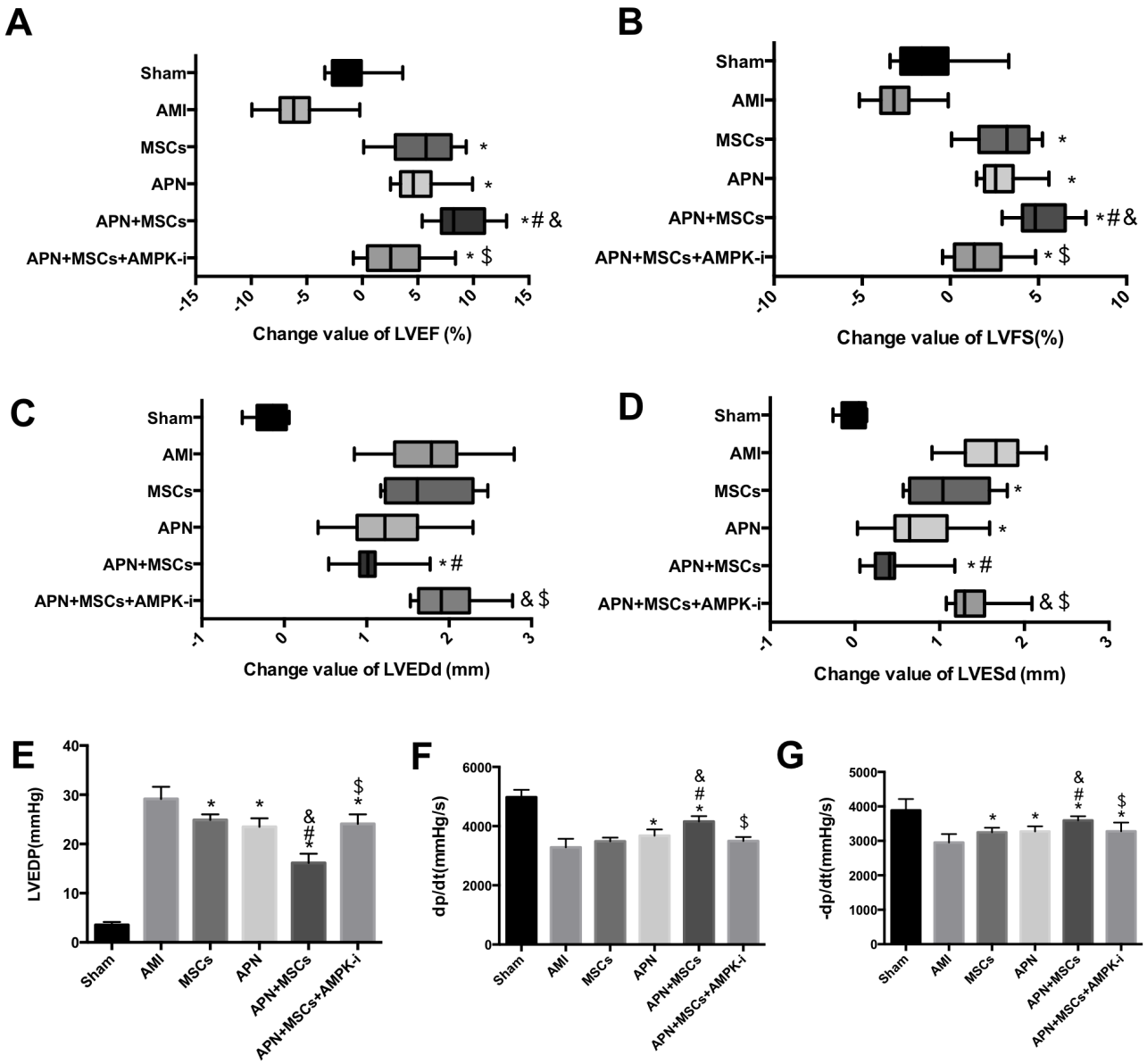

Figure 2

Assessments of cardiac function with echocardiography and left heart catheterization. (A-D): The change values of LVEF, LVFS, LVEDd and LVESd from baseline (1-week post AMI) to endpoint (4-week post AMI). (E-G): The values of LVEDP, dp/dtmax and −dp/dtmax detected at endpoint, respectively. At the baseline, the LVEF, LVFS, LVEDd and LVESd did not differ between AMI rats in different groups. At the endpoint, the combination regimen of APN and MSCs demonstrated a significant improvement in LVEF, LVFS, dp/dtmax and −dp/dtmax, which was significantly abrogated with the treatment of AMPK inhibitor. The values of change in LVEDd (ΔLVEDd), LVESd (ΔLVESd) and LVEDP at the endpoint were all dramatically reduced in APN + MSCs group compared with those in MSCs-only group, which were significantly increased with the addition administration of AMPK inhibitor. n=10 for each group. * $p < 0.05$ compared with AMI group; # $p < 0.05$ compared with MSCs group; & $p < 0.05$ compared with APN group; $ $p < 0.05$ compared with APN + MSCs group. AMI: acute myocardial infarction; APN: adiponectin; MSCs:

mesenchymal stem cells; AMPK: adenosine monophosphate-activated protein kinase; LVEF: left ventricular ejection fraction; LVFS: left ventricular fractional shortening; LVEDd: left ventricular end-diastolic dimension; LVESd: left ventricular end-systolic dimension; LVEDP: left ventricular end-diastolic dimension; dp/dtmax: left ventricular pressure maximal rate of rise; −dp/dtmax : left ventricular pressure maximal rate of fall.

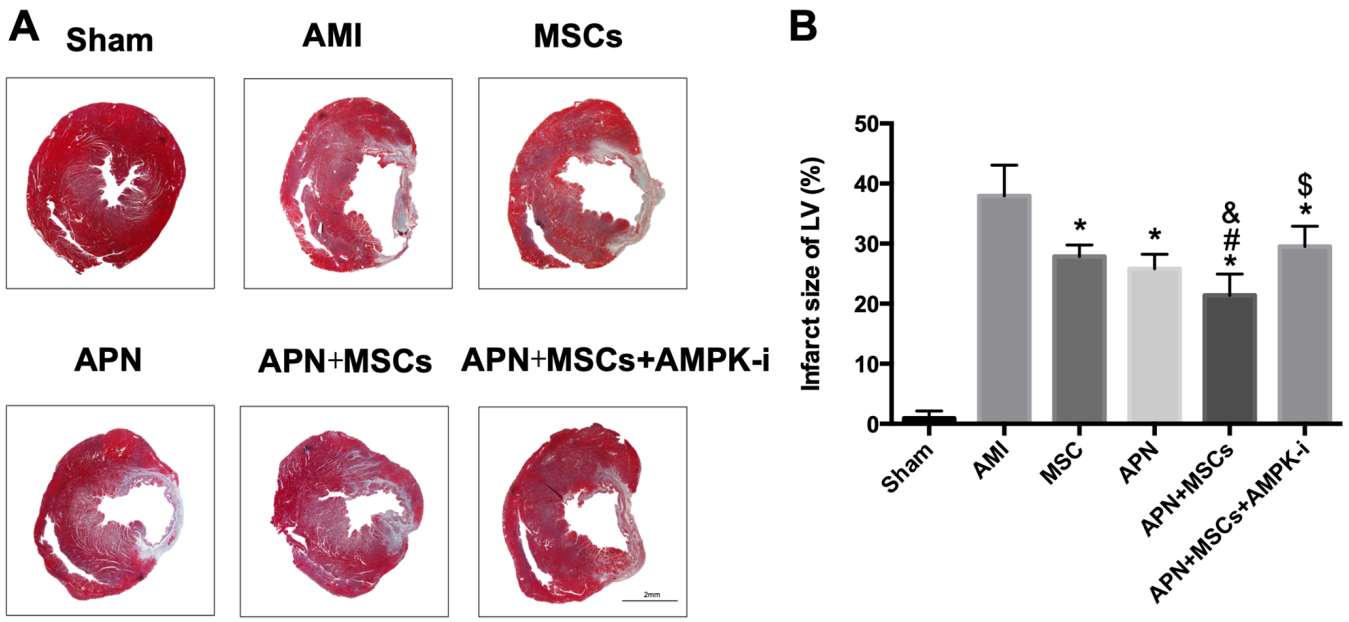

Figure 3

Measurement of left ventricular infarct size using Masson's trichrome staining. (A): Representative images of Masson's trichrome staining in each group. (B): Quantitative data for the left ventricular infarct size. Compared to all other group, the APN + MSCs group had the smallest infarct size, which was significantly reversed with the treatment of AMPK inhibitor. n = 10 in each group. * $p < 0.05$ compared with AMI group; # $p < 0.05$ compared with MSCs group; & $p < 0.05$ compared with APN group; $ $p < 0.05$ compared with APN + MSCs group. AMI: acute myocardial infarction; APN: adiponectin; MSCs: mesenchymal stem cells; AMPK: adenosine monophosphate-activated protein kinase. Scale bar = 2 mm.

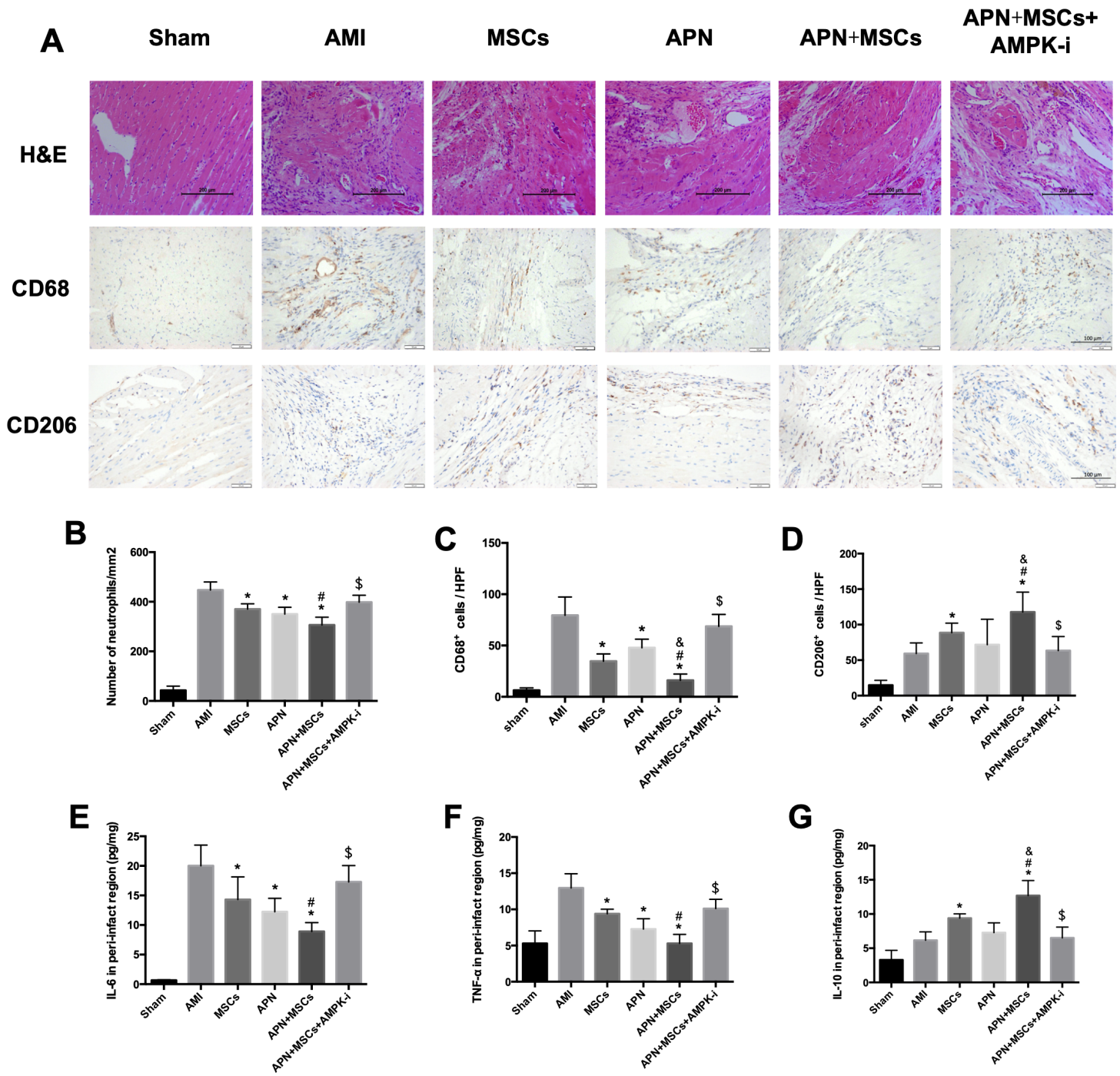

Figure 4

Assessments of inflammatory response in each group. (A): Representative images of H&E staining, CD68 and CD206 immunohistochemistry in each group (×200). (B): Quantitative data for the infiltration of neutrophils. (C, D): Quantitative data for the number of CD68+ and CD 206+ macrophages. APN + MSCs significantly reduced infiltration of neutrophils and CD 68+ macrophages, while increased the number of CD206+ macrophages. These effects were significantly reversed with the treatment of AMPK inhibitor. (E-G): Measurement of IL-6, TNF-α and IL-10 expressions in the peri-infarct myocardium with ELISA. APN +

MSCs significantly reduced pro-inflammatory cytokines IL-6 and TNF-α, while increased the level of anti-inflammatory cytokine IL-10. These effects were significantly reversed with the treatment of AMPK inhibitor. n=10 in each group. * $p < 0.05$ compared with AMI group; # $p < 0.05$ compared with MSCs group; & $p < 0.05$ compared with APN group; $ $p < 0.05$ compared with APN + MSCs group. AMI: acute myocardial infarction; APN: adiponectin; MSCs: mesenchymal stem cells; AMPK: adenosine monophosphate-activated protein kinase; IL: interleukin; TNF: tumor necrosis factor. Scale bar = 200 μm (H&E), 100 μm (CD68, CD206).

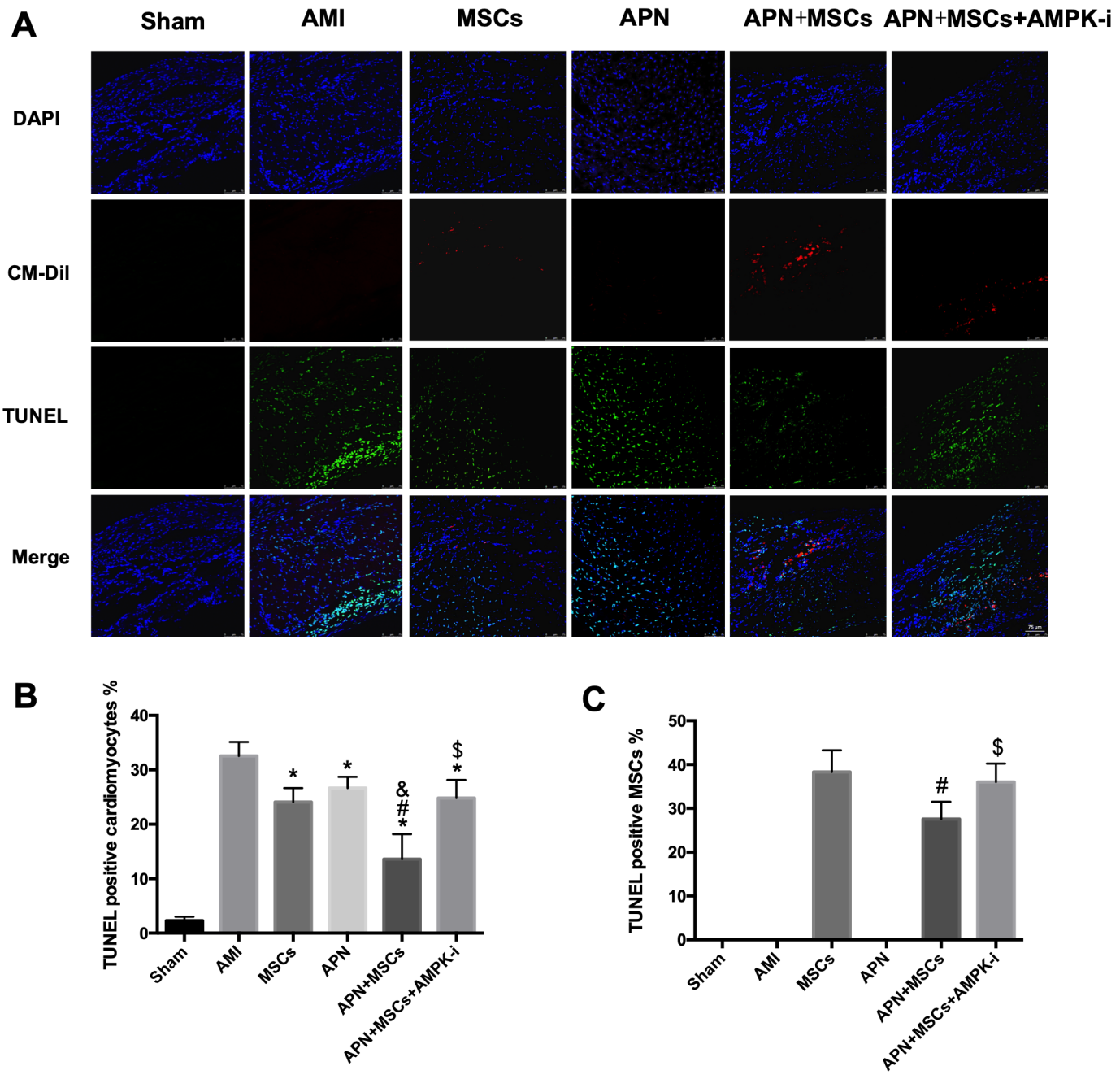

Figure 5

Assessments of cardiomyocytes and MSCs' apoptosis using TUNEL staining. (A): Representative images of TUNEL staining in each group (×200). (B): Ratio of apoptotic cardiomyocytes to total cells in each group. (C): Ratio of apoptotic MSCs to total cells in each group. APN + MSCs group induced a significant reduction in apoptotic cardiomyocytes and MSCs, both of which were significantly reversed with the treatment of AMPK inhibitor. * $p < 0.05$ compared with AMI group; # $p < 0.05$ compared with MSCs group; & $p < 0.05$ compared with APN group; $ $p < 0.05$ compared with APN + MSCs group. AMI: acute myocardial infarction; APN: adiponectin; MSCs: mesenchymal stem cells; AMPK: adenosine monophosphate-activated protein kinase. CM-DiI: 1,1'-dioctadecyl-3,3,3',3'-tetramethylindocarbocyanine perchlorate; DAPI: 4'6-diamidino-2-phenylindole dihydrochloride; TUNEL: TdT-mediated dUTP nick-end labeling. Scale bar = 75 μm.

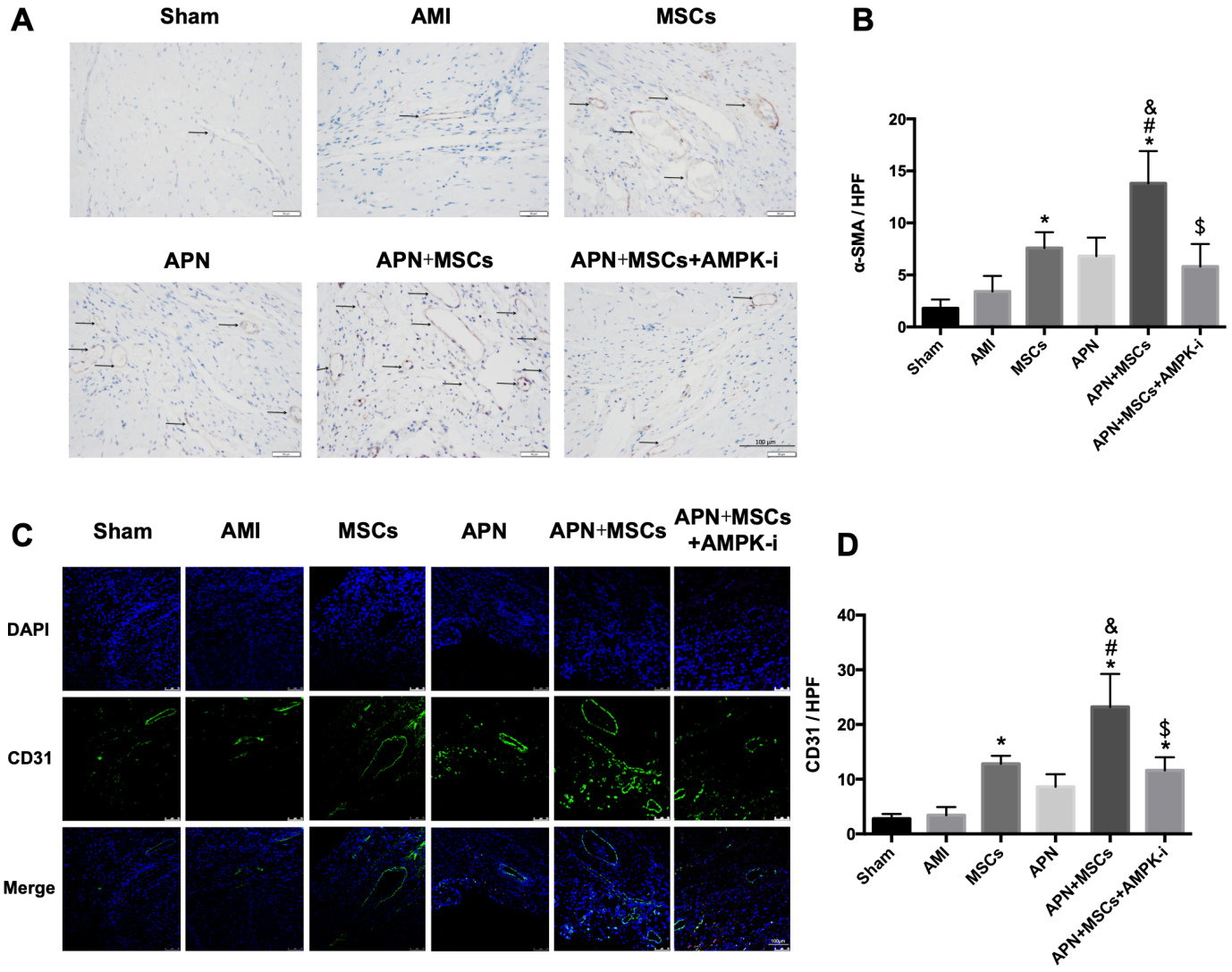

Figure 6

Arteriogenesis and angiogenesis evaluated by α-SMA and CD31 staining. (A): Representative images of α-SMA staining in peri-infarct myocardium in each group. Arrow: α-SMA positive vessels. (B): Arteriogenesis

was evaluated with number of α-SMA positive vessels per HPF. (C): Representative images of CD31 staining in peri-infarct myocardium in each group. (D): Angiogenesis was evaluated with number of CD31 positive vessels per HPF. APN + MSCs significantly increased ateriogenesis and angiogenesis compared with MSCs alone, which was significantly reversed with the treatment of AMPK inhibitor. * $p < 0.05$ compared with AMI group; # $p < 0.05$ compared with MSCs group; & $p < 0.05$ compared with APN group; $ $p < 0.05$ compared with APN + MSCs group. AMI: acute myocardial infarction; APN: adiponectin; MSCs: mesenchymal stem cells; AMPK: adenosine monophosphate-activated protein kinase; DAPI: 4'6-diamidino-2-phenylindole dihydrochloride; α-SMA, α-smooth muscle actin. Scale bar = 100 μm.

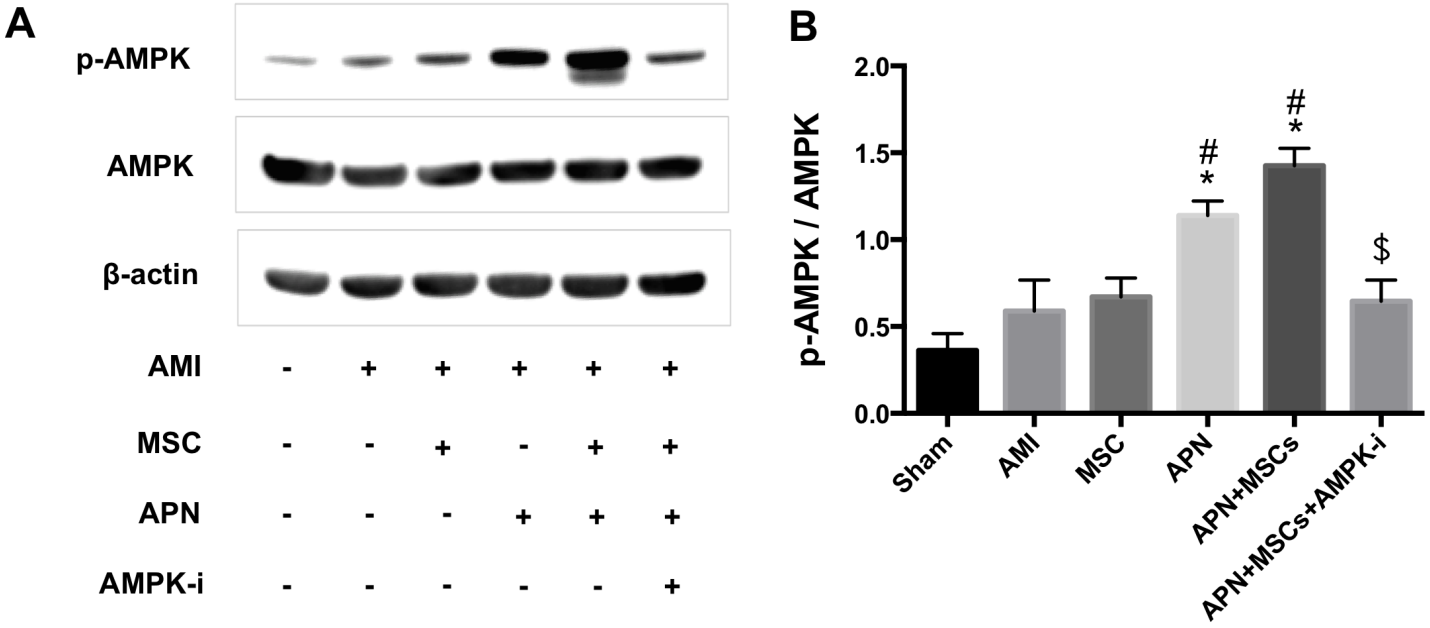

Figure 7

AMPK phosphorylation was assessed with Western blot. (A): Representative images of p-AMPK and AMPK expressions in each group. (B): Quantitative data for the p-AMPK / AMPK in each group. APN significantly increased the phosphorylation of AMPK in the myocardium. The combined therapy with APN and MSCs further activated AMPK phosphorylation, which could be markedly reversed by AMPK inhibitor. * $p < 0.05$ compared with AMI group; # $p < 0.05$ compared with MSCs group; & $p < 0.05$ compared with APN group; $ $p < 0.05$ compared with APN + MSCs group. AMI: acute myocardial infarction; APN: adiponectin; MSCs: mesenchymal stem cells; AMPK: adenosine monophosphate-activated protein kinase.

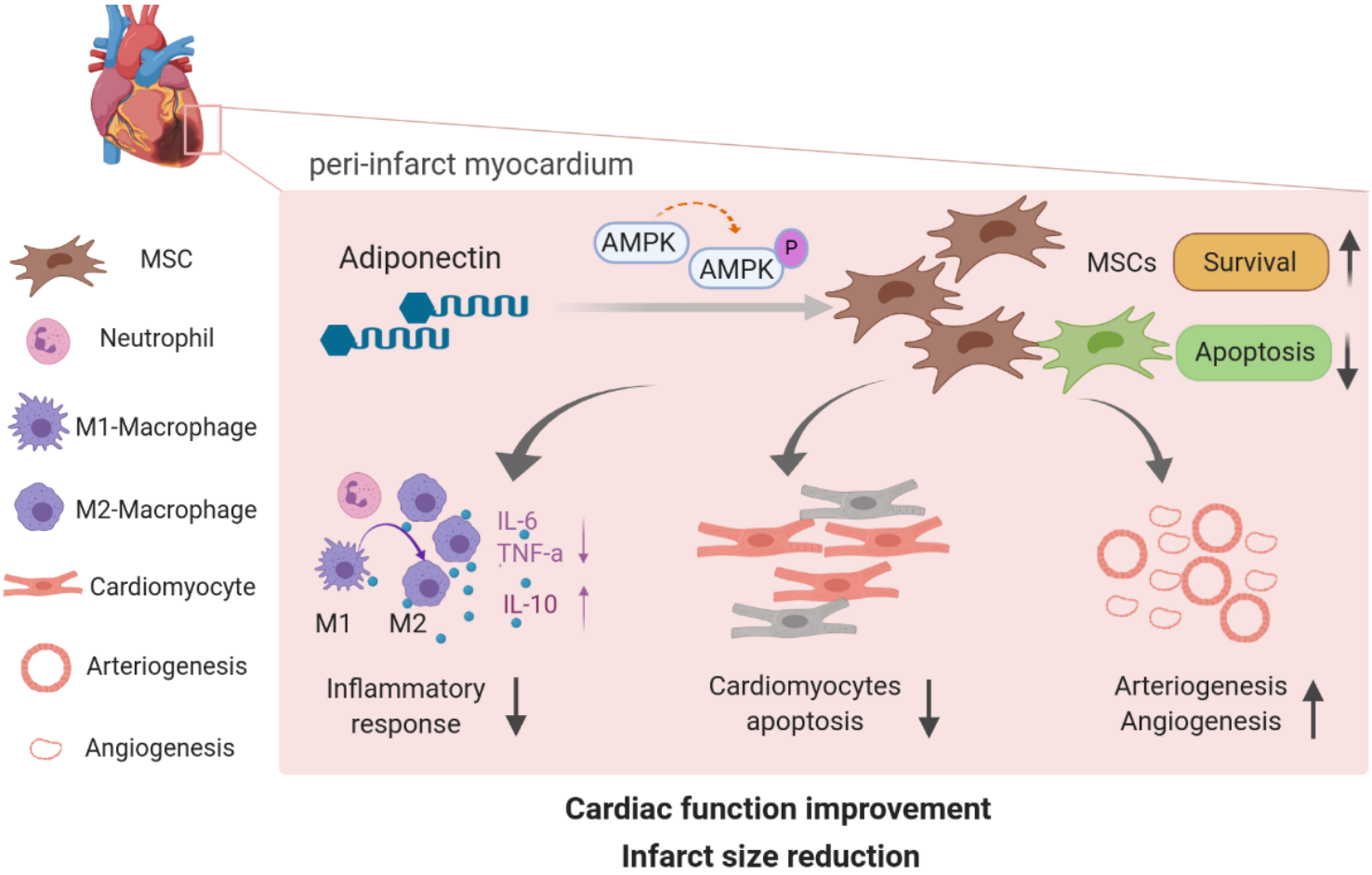

Figure 8

Schematic diagram of APN effects on MSCs survival and therapeutic efficacy in AMI. Adiponectin (APN) enhances the survival rate of transplanted mesenchymal stem cells (MSCs) via the activation of AMPK pathway. This augments the cardioprotective effects of MSCs on suppressing inflammatory response, inhibiting cardiomyocytes apoptosis, and enhancing arteriogenesis and angiogenesis in the peri-infarct myocardium. These beneficial effects further results in markedly improved cardiac function and decreased infarct size after acute myocardial infarction.

Supplementary Files

This is a list of supplementary files associated with this preprint. Click to download.

- SupplementalTables1.pdf